Supporting Information

Coupling of Triporosity and Strong Au-Li Interaction to Enable Dendrite-Free Lithium Plating/Stripping for Long-Life Lithium Metal Anodes

Yaohua Liang[a,b,1], Yuanmao Chen[a,b,1], Xi Ke[a,b,*], Zouxin Zhang[a,b], Wenli Wu[a,b], Guide Lin[a,b], Zhen Zhou[c] and Zhicong Shi[a,b,*]

[a] Smart Energy Research Centre, School of Materials and Energy, Guangdong University of Technology, Guangzhou 510006, China

[b] Guangdong Engineering Technology Research Center for New Energy Materials and Devices, Guangzhou 510006, China

[c] School of Materials Science and Engineering, Institute of New Energy Material Chemistry, Renewable Energy Conversion and Storage Center (ReCast), Key Laboratory of Advanced Energy Materials Chemistry (Ministry of Education), Nankai University, Tianjin 300350, China

* Corresponding author:
E-mail: kexi@gdut.edu.cn (X. Ke), zhicong@gdut.edu.cn (Z. Shi)

[1] Y.H. Liang and Y.M. Chen contributed equally to this work.

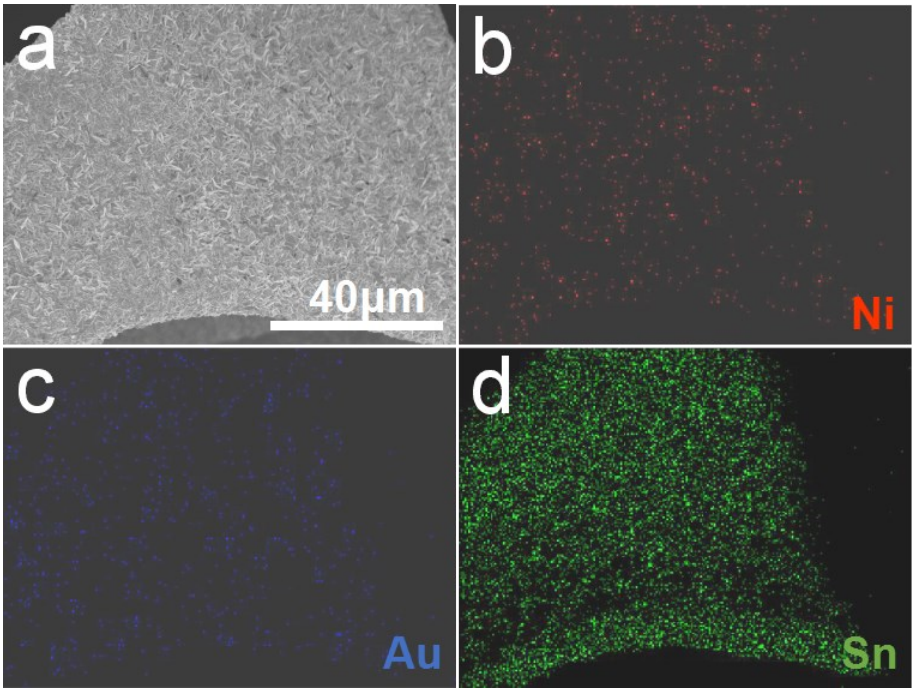

Figure S1. SEM image of AuSn@NF electrode (a) and the corresponding EDX elemental mapping images of Ni (b), Au (c) and Sn (d).

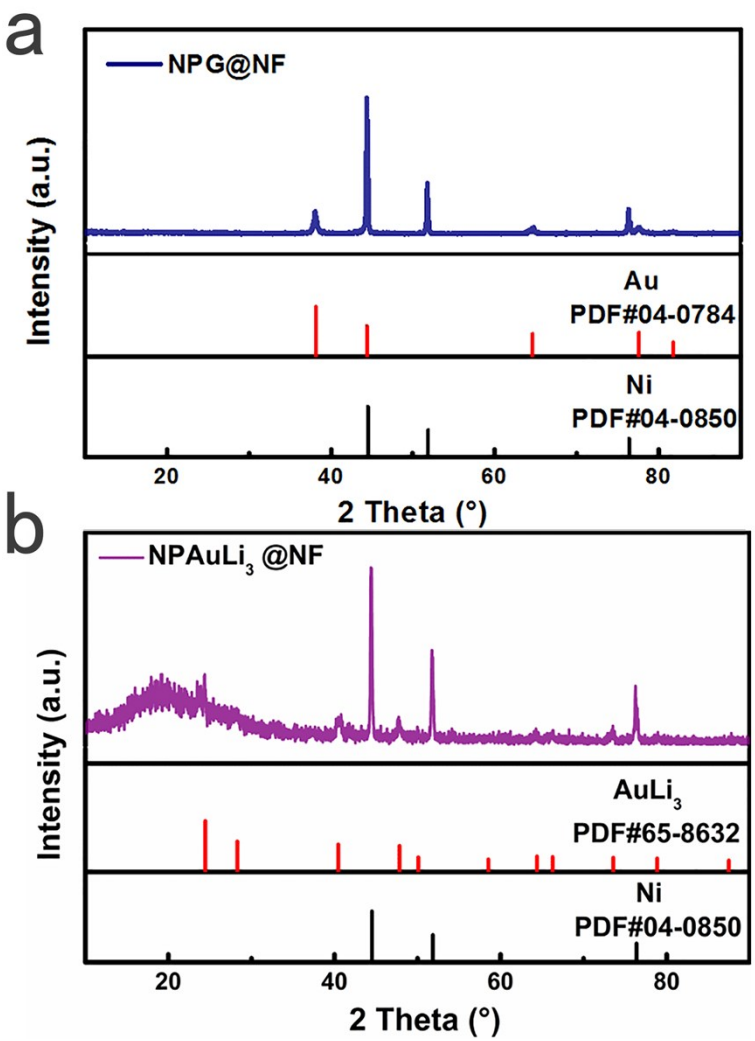

Figure S2. XRD patterns of NPG@NF (a) and NPAuLi$_3$@NF (b) electrodes.

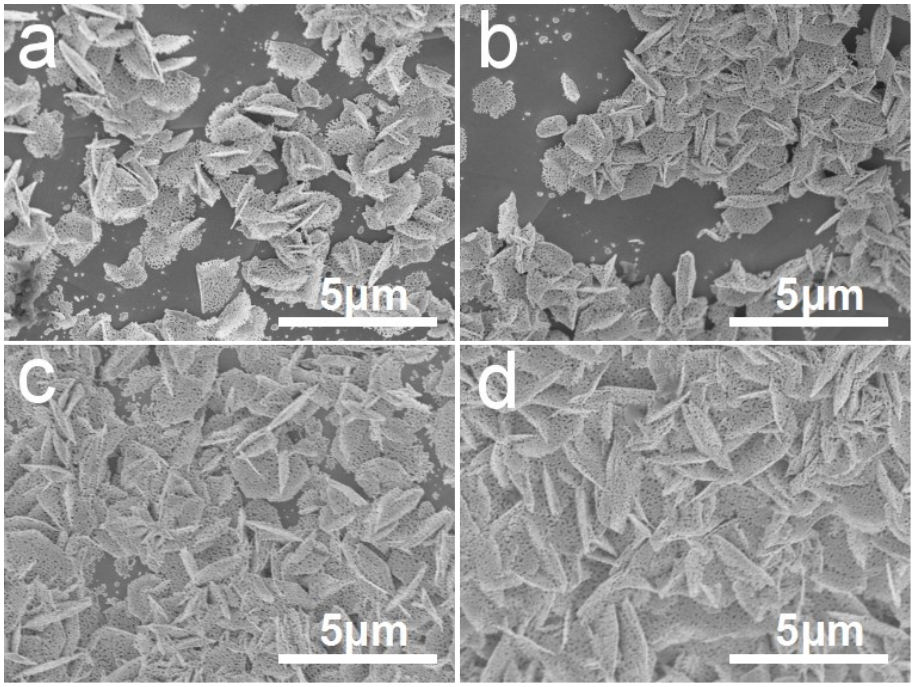

Figure S3. SEM images of NPG@NF obtained by chemically dealloying AuSn@NF electrodes electrodeposited at a current density of 5 mA cm^{-2} for 600 (a), 900 (b), 1050 (c) and 1200 (d) s, respectively.

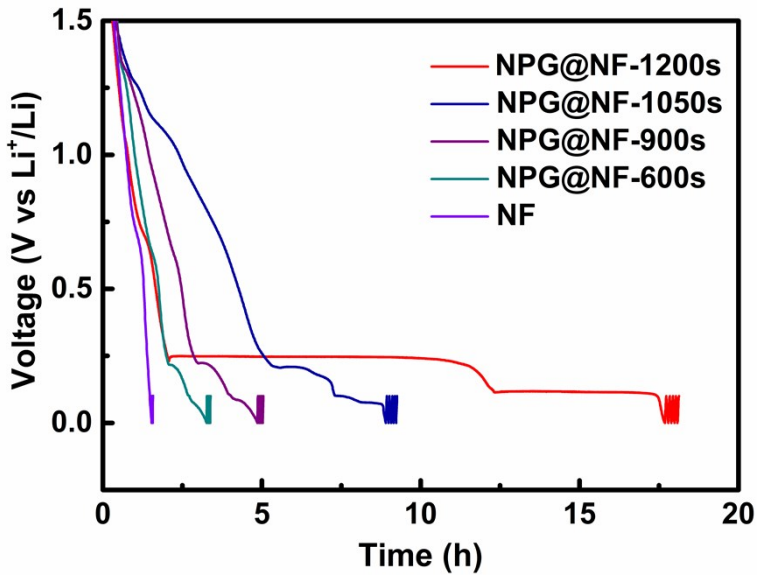

Figure S4. Voltage profiles of a galvanostatic discharge process to 0 V (vs. Li^+/Li) followed by a cycling between 0 and 0.1 V for 5 cycles at a current density of 50 μA cm^{-2} for NF and NPG@NF electrodes. NPG@NF electrodes were obtained by chemically dealloying AuSn@NF electrodes electrodeposited at a current density of 5 mA cm^{-2} for 600 (NPG@NF-600s), 900 (NPG@NF-900s), 1050 (NPG@NF-1050s) and 1200 (NPG@NF-1200s) s, respectively.

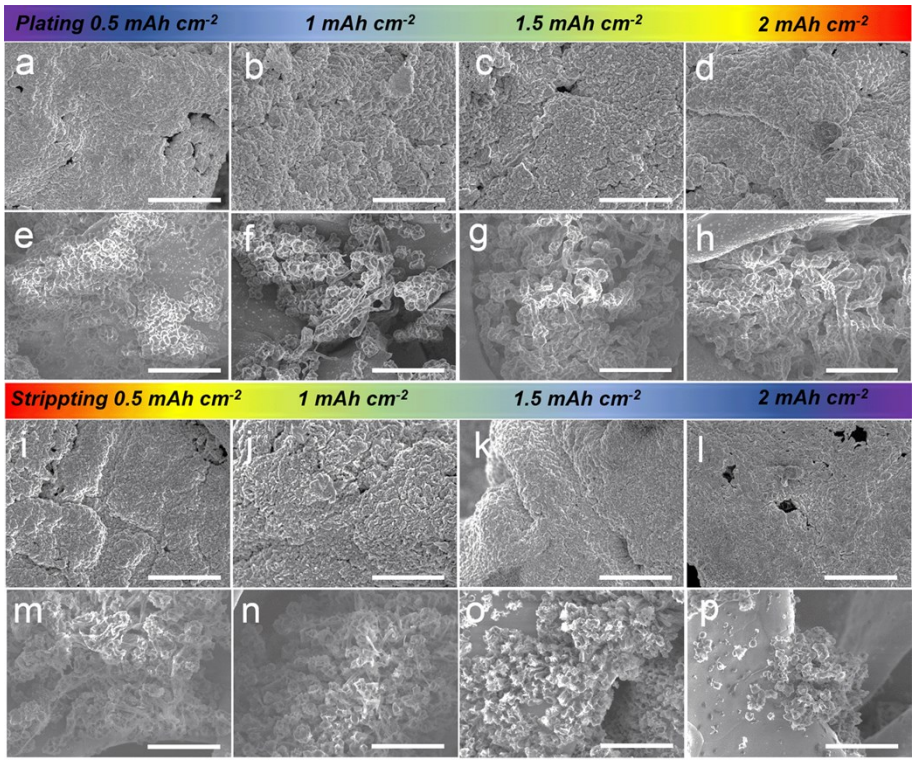

Figure S5. SEM images of $NPAuLi_3$@NF (a-d, i-l) and pristine NF (e-h, m-p) electrodes after plating 0.5 (a, e), 1 (b, f), 1.5 (c, g) and 2 (d, h) mAh cm^{-2} Li, and after stripping 0.5 (i, m), 1 (j, n), 1.5 (k, o) and 2 (l, p) mAh cm^{-2} Li, respectively, at a current density of 0.5 mA cm^{-2}. Scale bars: 20 μm.

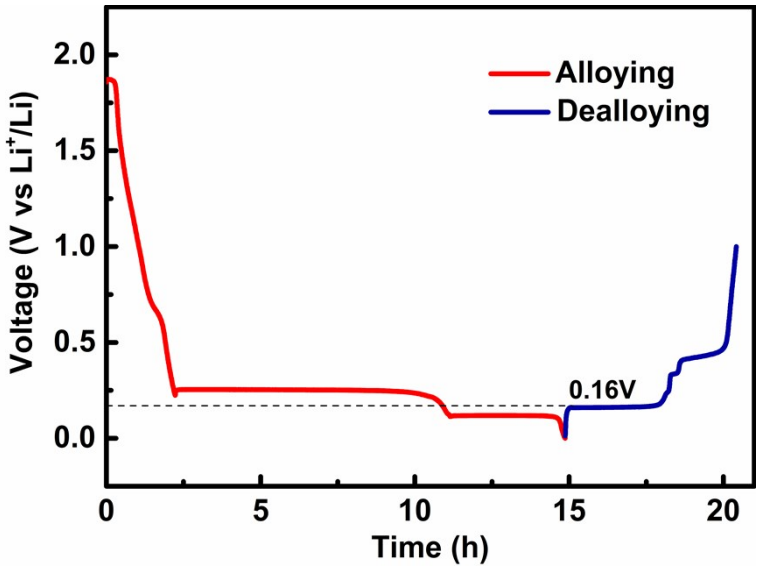

Figure S6. A representative voltage profile of the first discharge/charge cycle for a NPG@NF electrode at a current density of 50 μA cm^{-2}.

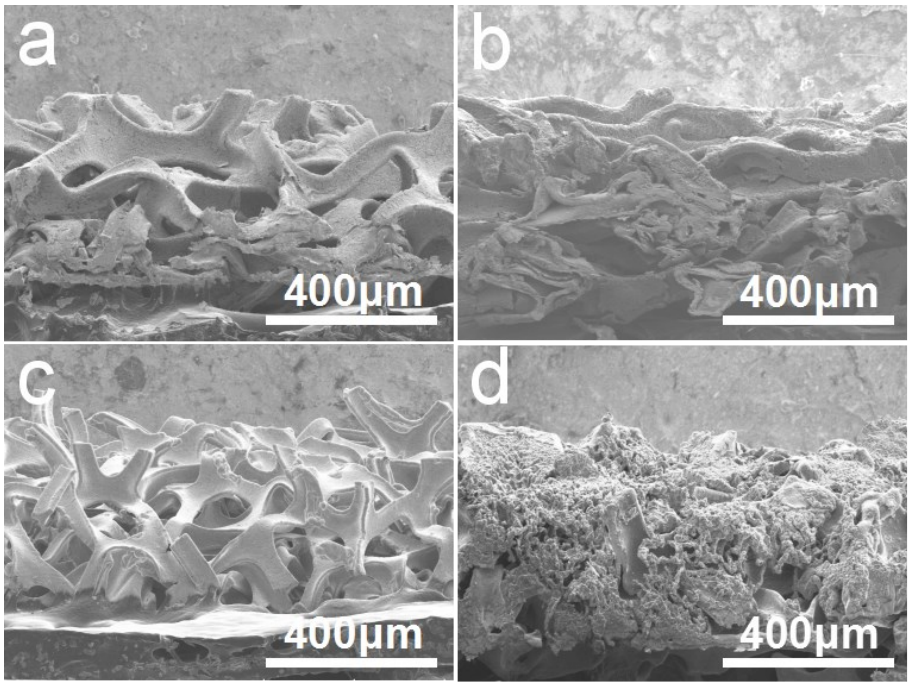

Figure S7. Cross-sectional SEM images of $NPAuLi_3$@NF (a, b) and NF (c, d) electrodes before (a, c) and after 50 (b, d) plating/stripping cycles at a current density of 1 mA cm^{-2} with a capacity of 2 mAh cm^{-2}.

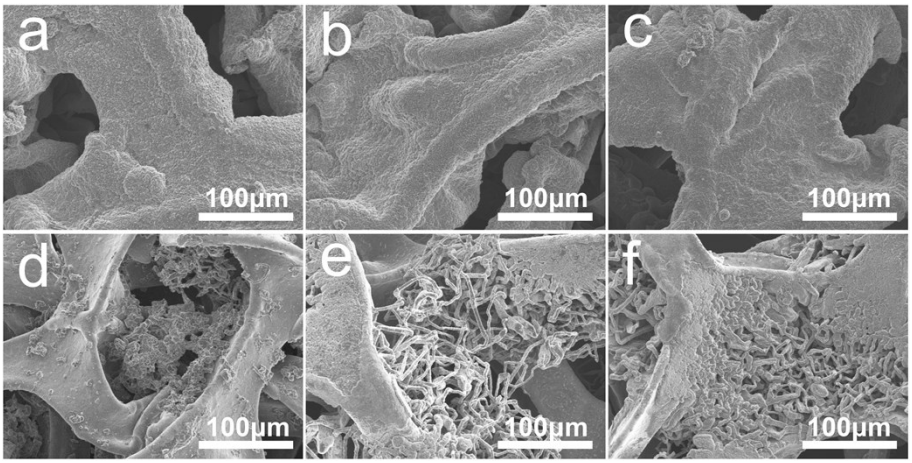

Figure S8. SEM images of the of the $NPAuLi_3$@NF (a-c) and bare NF (d-f) electrodes after 10 (a, d), 50 (b, e) and 100 (c, f) plating/stripping cycles, respectively, at a current density of 2 mA cm^{-2} with a capacity of 2 mAh cm^{-2}.

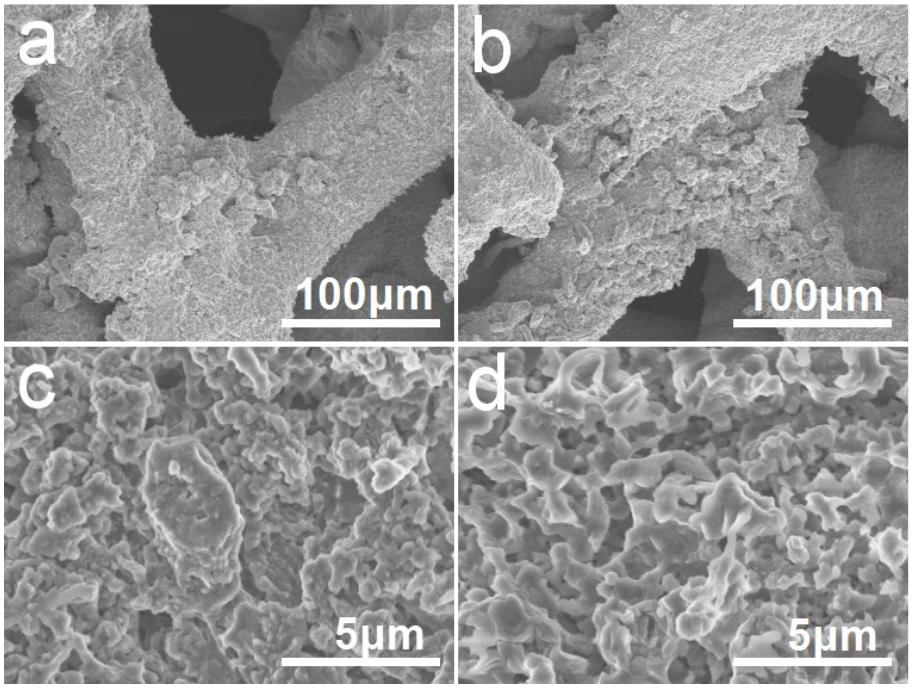

Figure S9. SEM images of $NPAuLi_3$@NF electrode after 10 (a, c) and 50 (b, d) plating/stripping cycles under an upper cutoff voltage of 1.0 V at a current density of 1 mA cm^{-2} with a capacity of 2 mAh cm^{-2}.

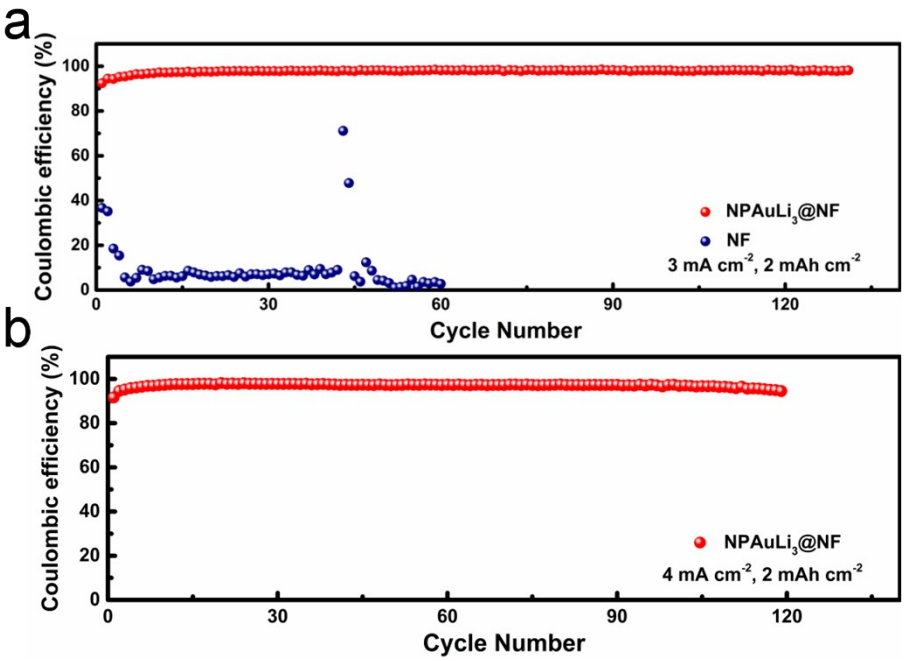

Figure S10. Coulombic efficiencies (CEs) for Li plating/stripping cycling on $NPAuLi_3$@NF (a, b) and NF (a) electrodes at current densities of 3 (a) and 4 (b) mA cm^{-2} with a capacity of 2 mAh cm^{-2}.

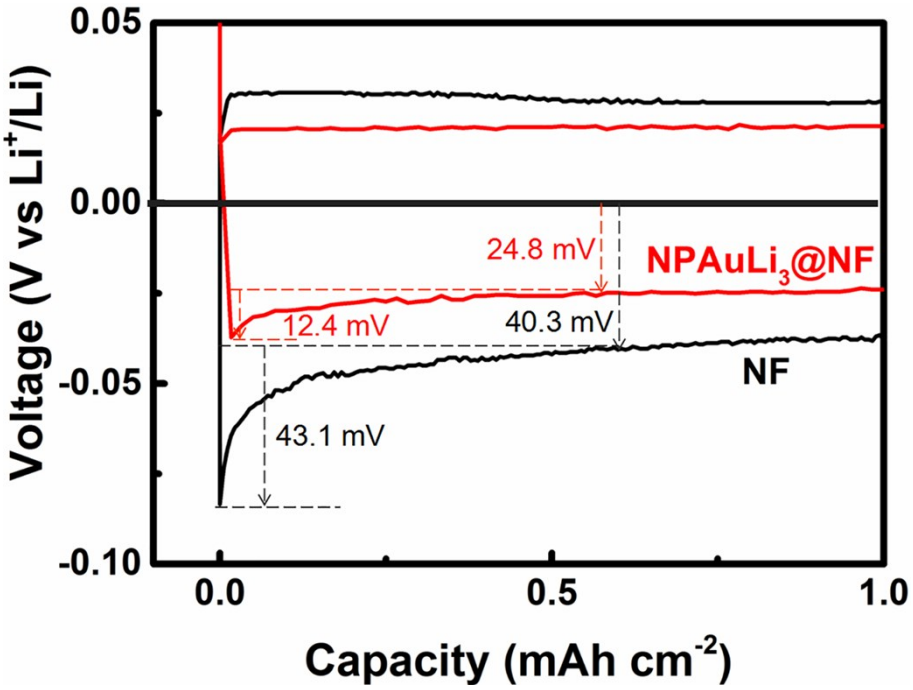

Figure S11. Voltage profiles of galvanostatic Li deposition on bare NF and $NPAuLi_3$@NF current collectors, respectively, at a current density of 1 mA cm^{-2}.

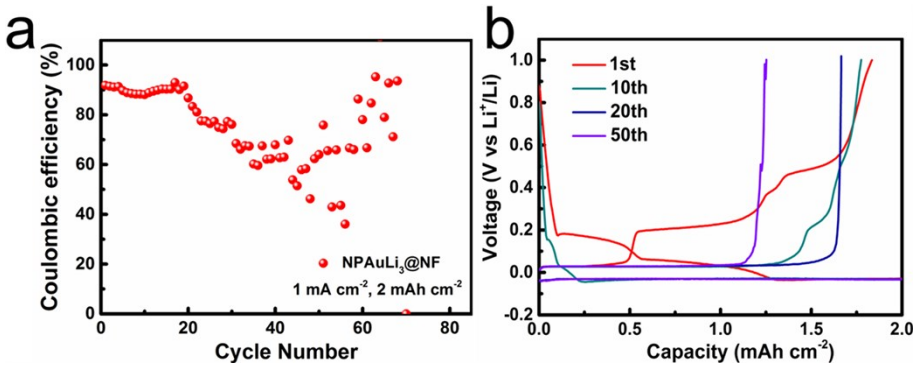

Figure S12. CE (a) and voltage profiles (b) for Li plating/stripping cycles on the $NPAuLi_3$@NF electrode under an upper cutoff voltage of 1.0 V at a current density of 1 mA cm^{-2} with a capacity of 2 mAh cm^{-2}.

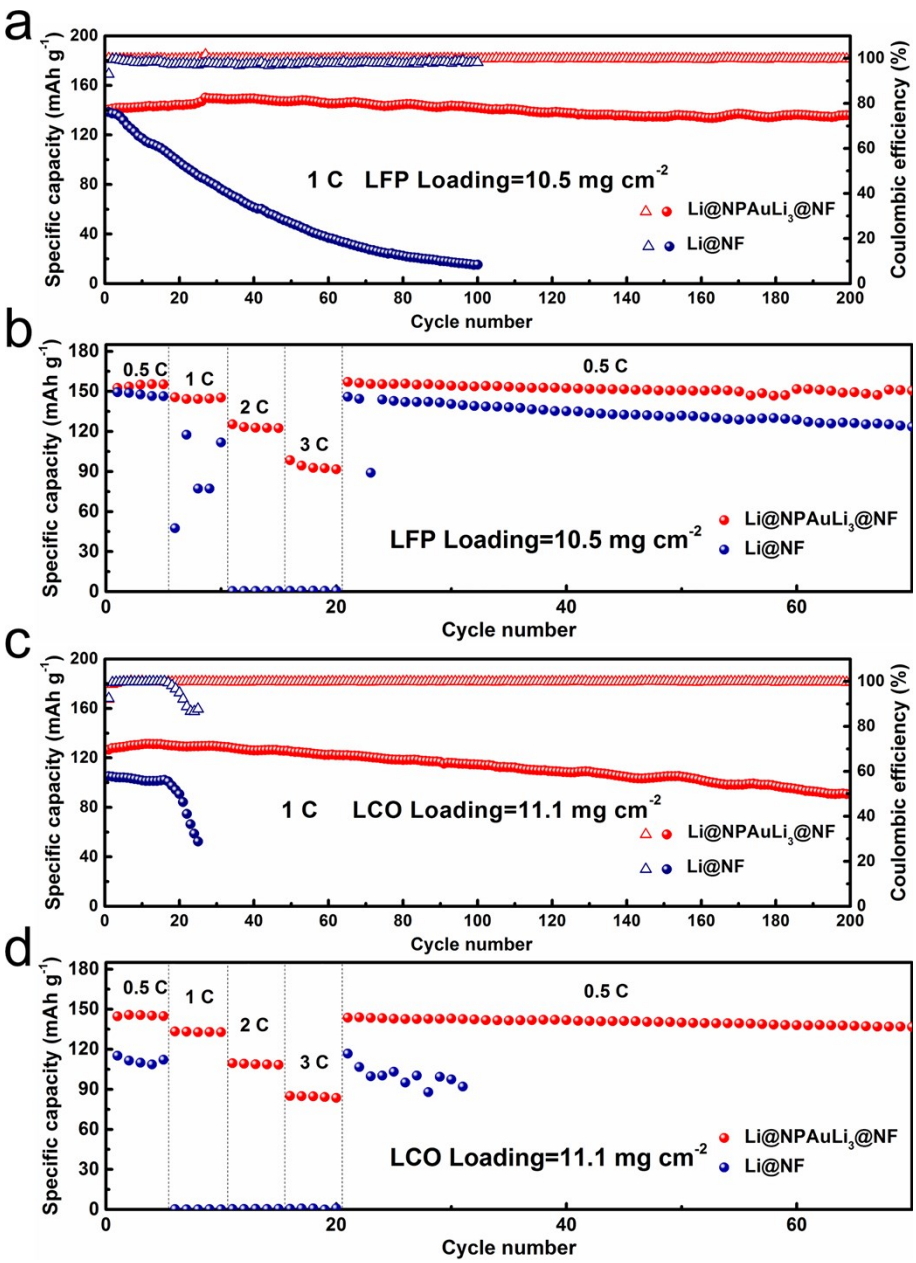

Figure S13. Cycling performance of LMAs with bare NF and $NPAuLi_3$@NF current collectors in full cells with a $LiFePO_4$ (LFP) (a) cathode with an areal mass loading of 10.5 mg cm^{-2}, and a $LiCoO_2$ (LCO) (c) cathode with an areal mass loading of 11.1 mg cm^{-2} at 1C. Rate capability of LMAs with bare NF and $NPAuLi_3$@NF current collectors in full cells with a LFP (b) and LCO (d) cathode at different rates from 0.5 to 3C.

Table S1. Calculation results of Li atom adsorption on $AuLi_3$ and NF slabs

Surface	Adsorption energies /eV	Adsorption site
Li-terminated $AuLi_3$ slab	-1.81	fcc
Au-terminated $AuLi_3$ slab	-2.29	fcc
NF slab	-1.23	fcc

Table S2. Coordination and bond length of the adsorbed Li atom on different slabs

Surface	Coordination number	Bond length /nm
Li-terminated $AuLi_3$ slab	3 Li atoms, 1 Au atom	0.297 (Li-Li) 0.265 (Li-Au)
Au-terminated $AuLi_3$ slab	3 Au atoms	0.2711 (Li-Au)
NF slab	3 Ni atoms	0.2556 (Li-Ni)

Table S3. Comparison of electrochemical performances of different LMAs in Li|Li symmetric cells

Anodes	Current density (mA cm^{-2})	Capacity (mAh cm^{-2})	Cycle time (h)	Ref.
Cu-CuO-Ni	0.5	0.5	580	1
3D Cu foil	0.2	1	1000	2
Cu@NPCN	0.5	1	1600	3
	1		1150	
NGCF@Li	2	1	1200	4
	3		600	
TiC/C/Li	1	1	400	5
	3		130	
Crumpled Graphene Balls@Li	0.5	1	750	6
AgNP/CNFs	0.5	1	500	7
GT scaffold	1	2	900	8
Li@CuCF	5	1	80	9
LNCO/Ni	1	1	1000	10
CNF-TiN	1	1	600	11
Li@Co_3N/NF	1	1	1100	12
Li/CuNW-P	1	1	1000	13
NPAuLi_3@NF	1	2	1990	This work
	2		1420	

References

1. S. L. Wu, Z. Y. Zhang, M. H. Lan, S. R. Yang, J. Y. Cheng, J. J. Cai, J. H. Shen, Y. Zhu, K. L. Zhang and W. J. Zhang, *Adv. Mater.*, 2018, **30**, 11705830.
2. Q. B. Yun, Y. B. He, W. Lv, Y. Zhao, B. H. Li, F. Y. Kang and Q. H. Yang, *Adv. Mater.*, 2016, **28**, 6932-6939.
3. F. Pei, A. Fu, W. B. Ye, J. Peng, X. L. Fang, M. S. Wang and N. F. Zheng, *ACS Nano*, **13**, 8337-8346.
4. L. Liu, Y. X. Yin, J. Y. Li, S. H. Wang, Y. G. Guo and L. J. Wan, *Adv. Mater.*, 2018, **30**, 1706216.
5. S. F. Liu, X. H. Xia, Y. Zhong, S. J. Deng, Z. J. Yao, L. Y. Zhang, X. B. Cheng, X. L. Wang, Q. Zhang and J. P. Tu, *Adv. Energy Mater.*, 2018, **8**, 1702322.
6. S. Liu, A. X. Wang, Q. Q. Li, J. S. Wu, K. Chiou, J. X. Huang and J. Y. Luo, *Joule*, 2018, **2**, 184-193.
7. C. P. Yang, Y. G. Yao, S. M. He, H. Xie, E. Hitz and L. B. Hu, *Adv. Mater.*, 2019, **29**, 1702714.
8. S. Jin, Z. W. Sun, Y. L. Guo, Z. K. Qi, C. K. Guo, X. H. Kong, Y. W. Zhu and H. X. Ji, *Adv. Mater.*, 2017, **29**, 1700783.
9. K. Chen, R. Pathak, A. Gurung, K. M. Reza, N. Ghimire, J. Pokharel, A. Baniya, W. He, J. J. Wu, Q. Q. Qiao and Y. Zhou, *J. Mater. Chem. A*, 2020, DOI: 10.1039/C9TA11237E.
10. X. Huang, X. Y. Feng, B. Zhang, L. Zhang, S. C. Zhang, B. Gao, P. K. Chu and K. F. Huo, *ACS Appl. Mater. Interfaces*, 2019, **11**, 31824-31831.
11. K. Lin, X. Y. Qin, M. Liu, X. F. Xu, G. M. Liang, J. X. Wu, F. Y. Kang, G. H. Chen

and B. H. Li, *Adv. Funct. Mater.*, 2019, **29**, 1903229.

12. M. N. Lei, J. G. Wang, L. B. Ren, D. Nan, C. Shen, K. Y. Xie and X. R. Liu, *ACS Appl. Mater. Interfaces*, 2019, **11**, 30992-30998.

13. C. Zhang, R. Y. Lyu, W. Lv, H. Li, W. Jiang, J. Li, S. C. Gu, G. M. Zhou, Z. J. Huang, Y. B. Zhang, J. Q. Wu, Q. H. Yang and F. Y. Kang, *Adv. Mater.*, 2019, **31**, 1904991.